The Influence of Flexure Variation to Vibration-Assisted Micro-Milling Device by Using Finite Element Analysis

Libyawati, Wina
Mechanical Engineering Department, Universitas Indonesia

Kiswanto, Gandjar
Mechanical Engineering Department, Universitas Indonesia

Agung Shamsuddin Saragih
Mechanical Engineering Department, Universitas Indonesia

Tae Jo Ko
School of Mechanical Engineering, Yeungnam University

https://doi.org/10.5109/4794205

出版情報：Evergreen. 9 (2), pp.577-583, 2022-06. 九州大学グリーンテクノロジー研究教育センター
バージョン：

The Influence of Flexure Variation to Vibration-Assisted Micro-Milling Device by Using Finite Element Analysis

Wina Libyawati[1], Gandjar Kiswanto[1,*], Agung Shamsuddin Saragih[1], Tae Jo Ko[2]

[1]Mechanical Engineering Department, Universitas Indonesia, Depok, Indonesia

[2] School of Mechanical Engineering, Yeungnam University, Gyeongsangbuk-do, Gyeongsan-si, South Korea

* Author to whom correspondence should be addressed:
E-mail: gandjar_kiswanto@eng.ui.ac.id

(Received February 11, 2022; Revised June 20, 2022; accepted June 20, 2022).

Abstract: This paper presents a compact method to predict the amplitude displacement and evaluate the influence of flexure structure on the vibration-assisted micro-milling device.The voltage load and flexure dimension variation are applied to the Finite Element model to obtain the predicted amplitude displacement. The simulation results show that amplitude displacement increases linearly along with the voltage load, but the influence of flexure thickness shows a varying trend on the amplitude displacement. The method can predict the device's amplitude displacement and movement pattern and is suitable for determining the optimum design for the vibration-assisted micro-milling device.

Keywords: amplitude displacement; Finite Element; flexure; piezoelectric actuator; vibration-assisted micro-milling

1. Introduction

The micro-milling process development leads to vibration-assisted micro-milling. The vibration-assisted micro-milling has been proven through simulation and experiment studies in the past decade that it improved the machined surface quality on a wide range of material properties [1–6]. The tool path trajectory is the primary performance of vibration-assisted micro-milling. During its application, the tool path, which is a linear path, becomes zig-zag or elliptical during the machining process.[7–9]. It will cause interrupting cutting that ignites an additional cooling period. The piezoelectric actuator is the main component of the device, which is operated by setting up the amplitude displacement and frequency[10–13]. Flexure or beam structure works with the actuator to achieve the designated displacement [14–23].

During machining, the amplitude displacement output from the piezoelectric actuator ranges between 0-10 micrometres and works based on the actuator material properties[24,25]. Several studies show amplitude displacement can be measured using displacement sensor[26,27] or predicted using Finite Element Analysis (FEA)[28–31]. The measurement method is more accurate than the prediction ones, but this method requires high investment in the micro displacement sensor and the ultrasonic-assisted micro-milling device prototype. The FEA method can predict the character and behaviour of the vibration-assisted micro-milling device at the early stage of design procedures. However, the FEA method, which considers the electromechanical constitutive model for the piezoelectric actuator material and the flexure characteristic, is limited to only a specific actuator.

The technology development for the micro-milling process and the actuator requires a compact method to achieve an optimum design of vibration-assisted micro-milling. Linear dynamic simulation is a solution to form a method because the amplitude displacement from the actuator is transmitted to flexure in the induction force[32]. Therefore, the amplitude displacement can be predicted with a compact method to achieve optimum design and suppress the experimental cost. Also, at the same time, the method can investigate the influence of the energy source to trigger the piezoelectric actuator and its component.

2. Methodology

Force calculation and linear dynamic simulation are the applied methodology for this study. The force calculation uses an analytical study by converting the voltage load from a single piezoelectric actuator into the induction forces[32]. The natural frequency of the piezoelectric actuator is simulated with modal analysis, as shown in Fig.1, based on its material properties, PZT4. The linear dynamic simulation uses the force calculation result as a part of the sinusoidal load function with the input parameter, as stated in Table 1. The induction force is applied in two directions to the head block components: on the feed and perpendicular to the feed direction.

The head block components use a flexure shape to transfer the induction force to the other components. Each end of the head block is set in the opposite direction of the phase. The phase difference is set to obtain the elliptical movement of the head block.

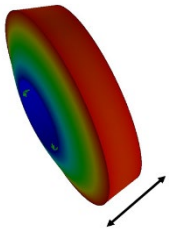

Fig. 1: Modal analysis of piezoelectric actuator at 167.25 kHz.

A CAD model is generated from Kiswanto et al.[33] vibration-assisted micro-milling for the simulation. Fig. 2 shows that the device employs two head blocks and flexure hinges. Also, each head block uses four piezoelectric actuators in a series arrangement. The input parameter is shown in Table 1 for the induction force calculation and linear dynamic simulation. The simulation in this paper is divided into two groups: voltage and flexure dimension variation base. All of the simulations are conducted with the aid of SOLIDWORKS.

Table 1. Input for voltage load and flexure dimension simulation.

Parameter	Value
Voltage	100;150;150 Volt
Piezoelectric actuator thickness	3 mm[33]
Strain constant	225x10^{-12} m/Volt
Permittivity constant	8.85 x 10^{-12} Farad/m[34]
Dielectric constant at -150 °C-250 °C	1000[34]
The operational frequency	24 kHz[33]
Phase	90°

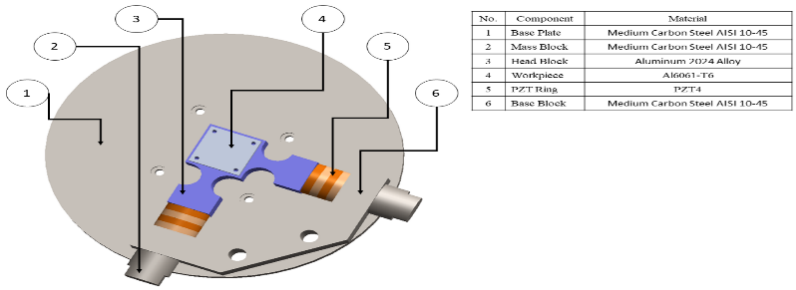

Fig. 2: CAD model vibration-assisted micro-milling device[33].

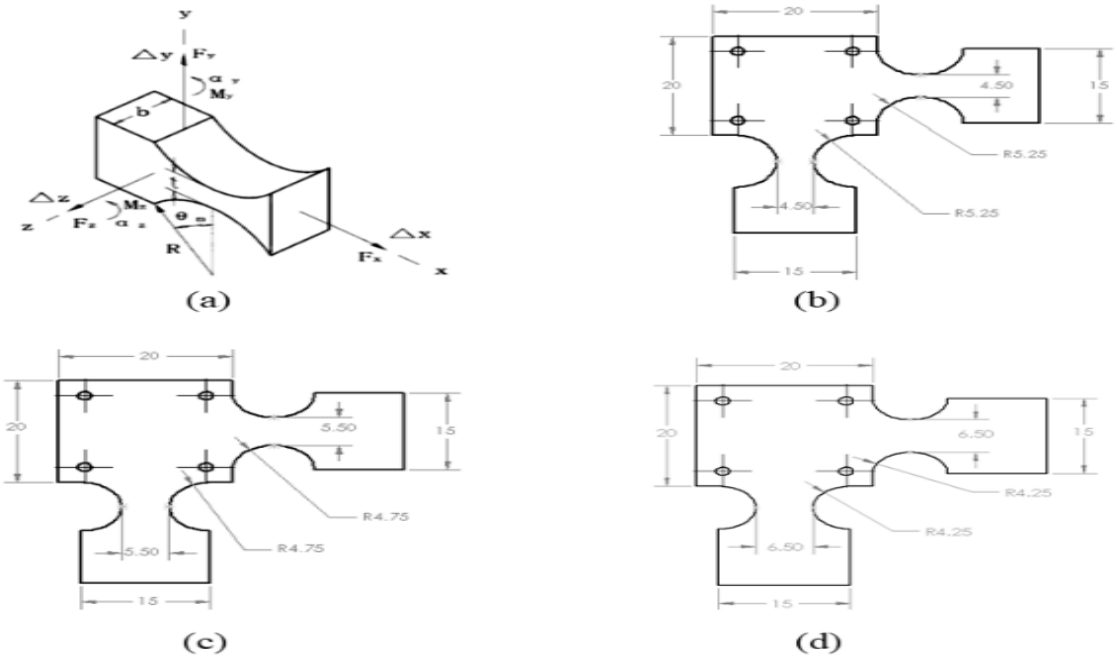

Fig. 3: Flexure dimension variation

The simulation-based on the voltage variation aims to investigate the voltage influence toward amplitude displacement of the vibration-assisted micro-milling device. The voltage load is variated into three loads in sequence 100, 150, and 200 Volt. The applied head block for the voltage variation uses a 5.5 mm thickness, as shown in Fig. 3(c). The converted induction forces from the voltage load are transformed into dynamic loads by considering the operational frequency, phase differences, and induction time. The time is set from zero to one second with an increment of 0.01 seconds from zero.

The simulation-based on flexure dimension variation aims to investigate the flexure dimension toward the amplitude displacement of the vibration-assisted micro-milling device. Fig. 3(a) shows the variated part of the flexure[14], which is the connector thickness between two segments(t). The thickness dimension is variated to 4.5, 5.5, and 6.5 mm, as shown in the sequence in Fig. 3(b)-3(d). The voltage is set constant at 100 volt for this simulation.

3. Result and Discussion

The induction force conversion from voltage load for one piezoelectric actuator is summarized in Table 2. Fig.4 shows the sinusoidal function's induction force with phase direction differences.

Table 2. Input for voltage load and flexure dimension simulation.

Load(Volt)	The force/ring PZT (N)	The Force in series (N)
100	1.72	6.88
150	2.857	10.348
200	3.45	13.8

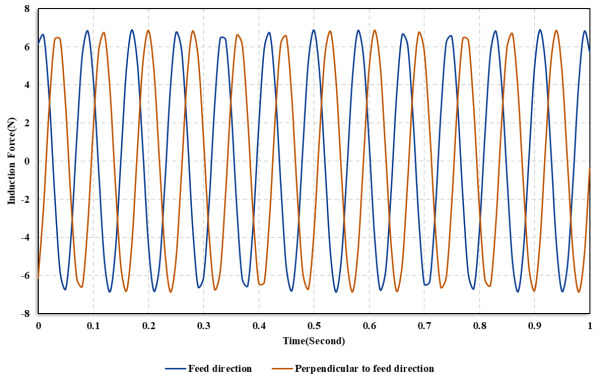

Fig. 4: The selected sinusoidal curve of induction force at 100 Volt at both flexure.

Fig.4 shows the induction force load at the feed and perpendicular to the feed direction. Therefore with the combined loads to the head block of the vibration-assisted micro-milling device, it experiences elliptical motion, as shown in Figure 5. The elliptical movement of the device will cause the cutting tool tip to move relatively with the same movement pattern as the device.

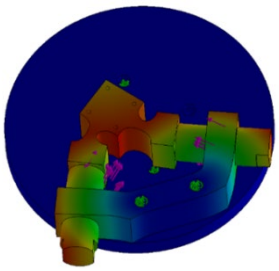

Fig. 5: The selected linear dynamic simulation result.

3.1 The influence of voltage variation

The series arrangement piezoelectric actuator is installed to induce the vibration-assisted micro-milling device, as shown in Fig. 6. The simulation result from the 100 Volt load represents the entire investigation of the voltage load influence to describe the device displacement at all axes. The resultant displacement output from the 100 Volt, as shown in Fig.6(a), ranges between 1×10^{-30} mm and 2.547×10^{-4} mm, and the head block experiences the amplitude displacement the most. The amplitude displacement simulation in Fig.6(b) and Fig.6(c) shows the amplitude displacement at the x-axis and y-axis (respectively, along the feed direction for the x-axis and the perpendicular to the feed direction for the y-axis) range between -2×10^{-4} mm-1.602×10^{-4} mm, which make the head block to experience elliptical motion. Small displacement in Fig.6(d) indicates that the displacement at the z-axis(respectively parallel to the tool) did not influence the device significantly.

The overall displacements from the linear dynamic simulation demonstrate that the voltage load resulted in micrometre displacement, which can develop a separation period between the tool and workpiece and achieve the targeted elliptical motion for the device. Both the micrometre displacement and an elliptical motion make the workpiece vibrate, which causes the tool to experience an elliptical tool path trajectory. The same procedures for the 100 Volt are used for the other voltage load. Afterwards, the finite element software calculates and records the output displacement and captures the average displacement.

The amplitude displacement of the vibration-assisted micro-milling device in Fig.7 increases with the voltage load and has an amplitude displacement below one micrometre. That simulation is the same as Zhang's study.[24]. The amplitude displacement of the device above one micrometre gives a more extended separation period between the tool and workpiece, but it requires a high energy source to produce voltage above 300 Volt. Re-designing the device also became another solution to achieve the targeted amplitude displacement and must consider material properties and the dimension of the entire device components.

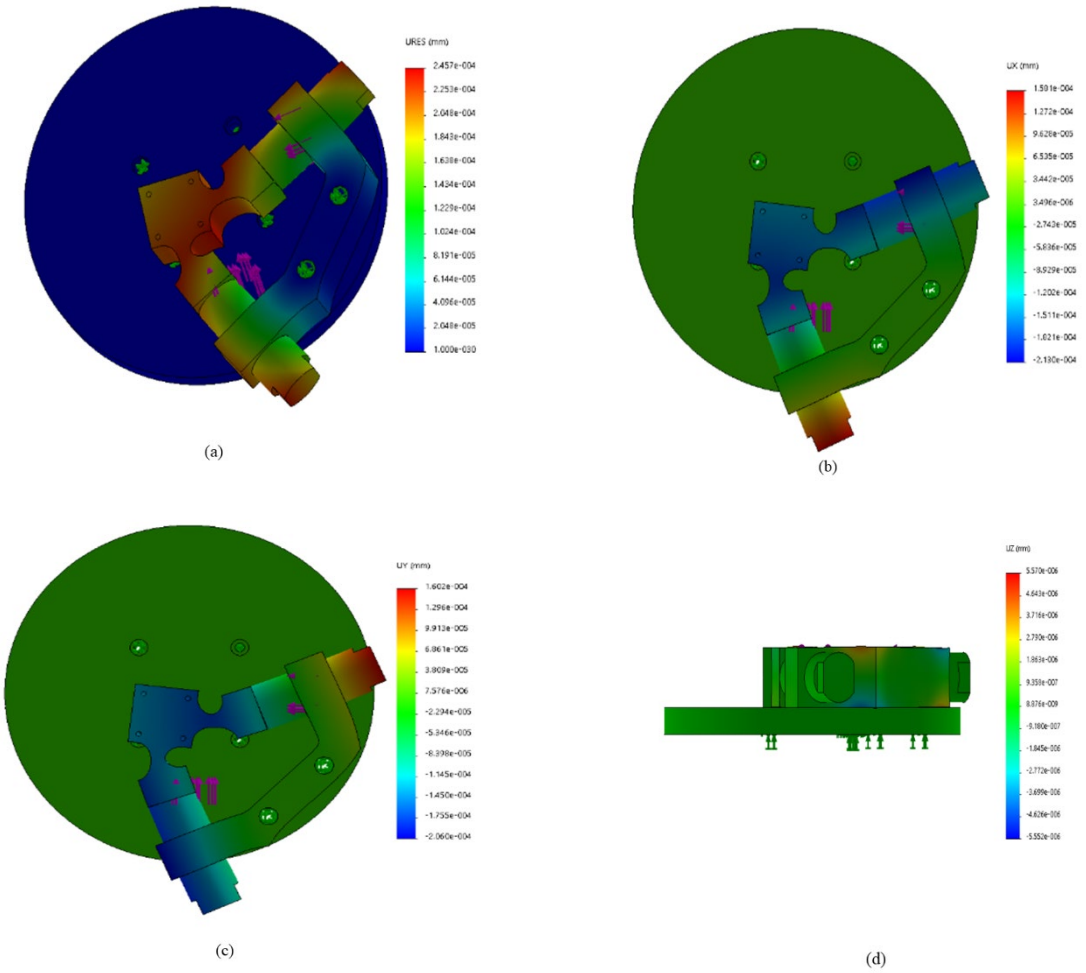

Fig. 6: The selected simulation result (a) (a) the resultant displacement, (b) displacement at the x-axis, (c) displacement at the y-axis, (d) displacement at z-axis.

3.2 The influence of flexure dimension

The results of the linear dynamic simulation at 200 Volt from the flexure thickness variation in Fig.8 show that the 5.5 mm flexure results in the highest displacement among the other flexure thickness. Fig.8 for the 5.5 and 6.5 mm thickness also displays dominant displacement at the machining x-y axis or feeding plane, compared to the displacement at the z-axis. The dominance amplitude displacement at the feeding plane indicates that the 5.5 and 6.5 mm flexure can produce an elliptical motion for the device and serve its function as a flexure hinge. So the 5.5 mm and 6.5 mm flexure can be adapted as the vibration-assisted micro-milling component. But for, the 4.5 mm thickness display dominance displacement at the z-axis. The dominance displacement at the z-axis is not applicable for the vibration-assisted micro-milling, which is placed in the feed direction, because it causes more friction between the tool and workpiece during machining. Also, the 4.5 mm appears to have high stiffness, so it can not serve its function as flexure. The repeated and high friction will speed up the tool wear. Therefore the 5.5 mm thickness is the most applicable flexure for this design as it results in the highest amplitude displacement. The simulation result also indicates that flexure variation influences investigation and should consider its critical dimensions.

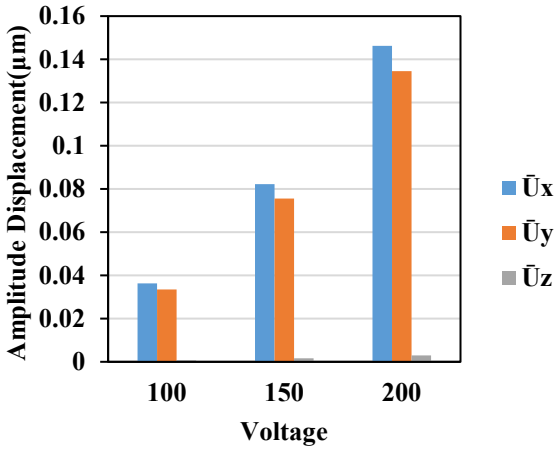

Fig. 7: The voltage load and amplitude displacement

The resultant amplitude displacement in Fig.9 shows that the piezoelectric actuator can superimpose the vibration-assisted micro-milling device with the 5.5 mm thickness flexure application. So it is chosen as the most optimum flexure for the vibration-assisted micro-milling device because it has the highest amplitude displacement. The 5.5 mm thickness flexure performance indicates that its thickness, length, and width allow the structure to deflect within micrometre displacement.

The chosen flexure design, which can apply an elliptical motion and operates below one-micrometre amplitude displacement, is applicable for vibration-assisted micro-milling installed at the feed direction. The device capability meets the specification of the device used by Ding et al.[11] and Jin et al.[13], and the application to the machining process improved the surface roughness below 10%. The influence of flexure as a component of vibration-assisted micro-milling had to be evaluated by considering voltage load, structure behaviour, and material properties to achieve the targeted amplitude displacement.

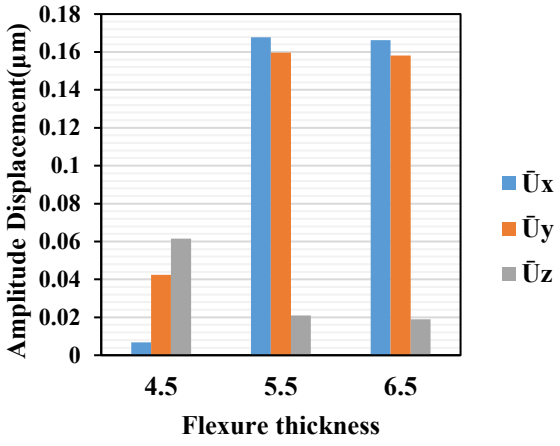

Fig. 8: The flexure and amplitude displacement for each axis

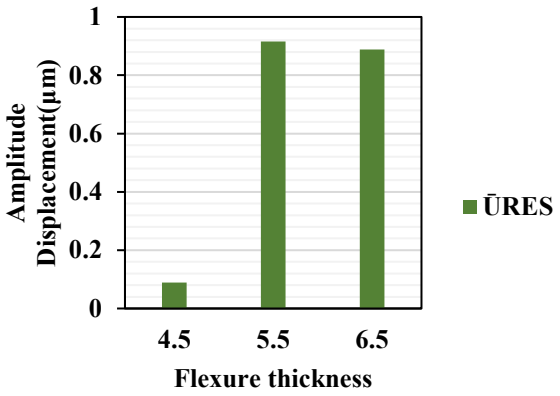

Fig. 9: The resultant displacement output from flexure variation

4. Conclusion

The voltage load and flexure thickness dimension variation influence the amplitude displacement of the vibration-assisted micro-milling device by using a compact method that considers the dielectric effect and with the aid of finite element software. The voltage load variation strongly influences the amplitude displacement, increasing linearly along with the voltage load. The flexure thickness dimension variation gives an un-trended influence to the amplitude displacement because the evaluation of flexure influence must include the entire flexure dimension. The method proved capable of predicting the amplitude displacement, choosing the optimum design of the vibration-assisted micro-milling, and describing the device movement relative to the tool. So, this method will ease the researcher to predict the amplitude displacement of the vibration-assisted micro-milling device and suppress the experimental cost. Further studies are required to investigate the characteristics of flexure influence on the amplitude displacement by considering structure dimensions and material properties as an integrated component of the vibration-assisted micro-milling device.

Acknowledgements

The Indonesian Ministry of Education, Culture, Research and Technology under the PDUPT "Penelitian Dasar Unggulan Perguruan Tinggi" grant scheme No. NKB-1637/UN2.R3.1/HKP.05.00/2019, sponsors this study.

References

1) L. Zheng, W. Chen, and D. Huo, "Review of vibration devices for vibration-assisted machining," *Int. J. Adv. Manuf. Technol.*, (2020). doi:10.1007/s00170-020-05483-8.
2) A.M. Rosli, A.S. Jamaludin, and M.N.M. Razali, "Recent study on hard to machine material – micromilling process," *Evergr. Jt. J. Nov. Carbon Resour. Sci. Green Asia Strateg.*, **08** (*02*) 445–453 (2021). http://hdl.handle.net/2324/4480727 (accessed December 12, 2021).
3) S.J. Zhang, S. To, G.Q. Zhang, and Z.W. Zhu, "A review of machine-tool vibration and its influence upon surface generation in ultra-precision machining," *Int. J. Mach. Tools Manuf.*, **91** 34–42 (2015). doi:https://doi.org/10.1016/j.ijmachtools.2015.01.005.
4) Y. Whulanza, A. Hakim, M. Utomo, R. Irwansyah, J. Charmet, and Warjito, "Design and characterization of finger-controlled micropump for lab-on-a-chip devices," *Evergreen*, **6** 108–113 (2019). doi:10.5109/2321002.
5) A. Srivastava, S. Dwivedi, N. Maurya, and M. Maurya, "3D visualization and topographical analysis

in turning of hybrid mmc by cnc lathe sprint 16tc made of batliboi," *Evergreen*, **7** 202–208 (2020). doi:10.5109/4055217.

6) A. Gupta, H. Kumar, L. Nagdeve, and P. Arora, "EDM parametric study of composite materials: a review," *Evergreen*, **7** 519–529 (2020). doi:10.5109/4150471.
7) X.-H. Shen, J.-H. Zhang, H. Li, J.-J. Wang, and X.-C. Wang, "Ultrasonic vibration-assisted milling of aluminum alloy," *Int. J. Adv. Manuf. Technol.*, **63** (*1*) 41–49 (2012). doi:10.1007/s00170-011-3882-5.
8) W. Chen, L. Zheng, W. Xie, K. Yang, and D. Huo, "Modelling and experimental investigation on textured surface generation in vibration-assisted micro-milling," *J. Mater. Process. Technol.*, **266** 339–350 (2019). doi:https://doi.org/10.1016/j.jmatprotec.2018.11.011.
9) W. Chen, D. Huo, J. Hale, and H. Ding, "Kinematics and tool-workpiece separation analysis of vibration assisted milling," *Int. J. Mech. Sci.*, **136** 169–178 (2018). doi:https://doi.org/10.1016/j.ijmecsci.2017.12.037.
10) S.Z. Chavoshi, and X. Luo, "Hybrid micro-machining processes: a review," *Precis. Eng.*, **41** 1–23 (2015). doi:https://doi.org/10.1016/j.precisioneng.2015.03.001.
11) H. Ding, R. Ibrahim, K. Cheng, and S.-J. Chen, "Experimental study on machinability improvement of hardened tool steel using two dimensional vibration-assisted micro-end-milling," *Int. J. Mach. Tools Manuf.*, **50** (*12*) 1115–1118 (2010). doi:https://doi.org/10.1016/j.ijmachtools.2010.08.010.
12) X.-H. Shen, and G.-F. Xu, "Study of milling force variation in ultrasonic vibration-assisted end milling," *Mater. Manuf. Process.*, **33** (*6*) 644–650 (2018). doi:10.1080/10426914.2017.1364846.
13) X. Jin, and B. Xie, "Experimental study on surface generation in vibration-assisted micro-milling of glass," *Int. J. Adv. Manuf. Technol.*, **81** (2015). doi:10.1007/s00170-015-7211-2.
14) Z. Wu, Yingfei,Zhou, "Design calculation for flexure hinge," *Rev. Sci. Instrum.*, **73** (*8*) 3101 (2002). doi:https://doi.org/10.1063/1.1494855.
15) F. Dirksen, and R. Lammering, "On mechanical properties of planar flexure hinges of compliant mechanisms," *Mech. Sci.*, **2** 109–117 (2011).
16) S. Xiao, Y. Li, and X. Zhao, "Design and analysis of a novel flexure-based XY micro-positioning stage driven by electromagnetic actuators," in: Proc. 2011 Int. Conf. Fluid Power Mechatronics, 2011: pp. 953–958. doi:10.1109/FPM.2011.6045900.
17) M. Liu, X. Zhang, and sergej fatikow, "Design and analysis of a high-accuracy flexure hinge," *Rev. Sci. Instrum.*, **87** 055106 (2016). doi:https://doi.org/10.1063/1.4948924.
18) B. Denkena, T. Grove, and A. Seibel, "Direct part marking by vibration assisted face milling," *Procedia Technol.*, **26** 185–191 (2016). doi:https://doi.org/10.1016/j.protcy.2016.08.025.
19) L. Zheng, W. Chen, D. Huo, and X. Lyu, "Design, analysis, and control of a two-dimensional vibration device for vibration-assisted micromilling," *IEEE/ASME Trans. Mechatronics*, **25** (*3*) 1510–1518 (2020). doi:10.1109/TMECH.2020.2978209.
20) G.D. Kim, and B.G. Loh, "Direct machining of micro patterns on nickel alloy and mold steel by vibration assisted cutting," *Int. J. Precis. Eng. Manuf.*, **12** (*4*) 583–588 (2011). doi:10.1007/s12541-011-0075-y.
21) X.-H. Shen, J. Zhang, D.X. Xing, and Y. Zhao, "A study of surface roughness variation in ultrasonic vibration-assisted milling," *Int. J. Adv. Manuf. Technol.*, **58** (*5*) 553–561 (2012). doi:10.1007/s00170-011-3399-y.
22) G.-L. Chern, and Y.-C. Chang, "Using two-dimensional vibration cutting for micro-milling," *Int. J. Mach. Tools Manuf.*, **46** (*6*) 659–666 (2006). doi:https://doi.org/10.1016/j.ijmachtools.2005.07.006.
23) G. Li, B. Wang, J. Xue, D. Qu, and P. Zhang, "Development of vibration-assisted micro-milling device and effect of vibration parameters on surface quality and exit-burr," *Proc. Inst. Mech. Eng. Part B J. Eng. Manuf.*, **233** (*6*) 1723–1729 (2018). doi:10.1177/0954405418774592.
24) P. Zhang, "Chapter 3 - Sensors and actuators," in: P.B.T.-A.I.C.T. Zhang (Ed.), William Andrew Publishing, Oxford, 2010: pp. 73–116. doi:https://doi.org/10.1016/B978-1-4377-7807-6.10003-8.
25) A.M. Halawa, B. Elhadidi, and S. Yoshida, "Aerodynamic performance enhancement using active flow control on du96-w-180 wind turbine airfoil," *Evergreen*, **5** (*1*) (2018). doi:10.5109/1929723.
26) K. Liang, C. Li, Y. Tong, J. Fang, and W. Zhong, "Design of a low-frequency harmonic rotary piezoelectric actuator," *Actuators*, **10** (*1*) (2021). doi:10.3390/act10010004.
27) W. Huang, J. Lian, M. Chen, and D. An, "Bidirectional active piezoelectric actuator based on optimized bridge-type amplifier," *Micromachines*, **12** (*9*) 1013 (2021). doi:10.3390/mi12091013.
28) Ibrahim, Rasidi, Rachmat, Haris, Dida, Damayanti, Radzi, Anis, and Mulyana, Tatang, "An investigation of finite element analysis (fea) on piezoelectric compliance in ultrasonic vibration assisted milling (uvam)," *MATEC Web Conf.*, **150** 4002 (2018). doi:10.1051/matecconf/201815004002.
29) L. Jieqiong, H. Jinguo, L. Mingming, G. Yan, and Z. Wenhui, "Development of nonresonant elliptical vibration cutting device based on parallel piezoelectric actuator," *AIP Adv.*, **7** (*3*) 035304 (2017).

doi:10.1063/1.4978262.

30) A.A. Shah, "FEM-bem interactive coupling for modeling the piezoelectric health monitoring systems.," *Lat. Am. J. Solids Struct.*, **8** (*3A*) 305–334 (2011). doi:https://doi.org/10.1590/S1679-78252011000300007.
31) A. Kumar, A. Chanda, and S. Angra, "Numerical modelling of a composite sandwich structure having non metallic honeycomb core," *Evergreen*, **8** 759–767 (2021). doi:10.5109/4742119.
32) E. Porcelli, and V. Filho, "Induction of forces performed by piezoelectric materials," *J. Power Energy Eng.*, **06** (2016). doi:10.4236/jpee.2018.61004.
33) G. Kiswanto, Poly, Y.R. Johan, T.J. Ko, and R. Kurniawan, "Development of langevin piezoelectric transducer-based two dimensional ultrasonic vibration assisted machining (2d {uvam}) on 5-axis micro-milling machine," *{IOP} Conf. Ser. Mater. Sci. Eng.*, **654** 12015 (2019). doi:10.1088/1757-899x/654/1/012015.
34) M.W. Hooker, "Properties of PZT-Based Piezoelectric Ceramics Between -150 and 250 C," 1998. https://ntrs.nasa.gov/citations/19980236888.